Membrane Permeabilization Induced by Sphingosine: Effect of Negatively Charged Lipids

Noemi Jiménez-Rojo,[†] Jesús Sot,[†] Ana R. Viguera,[†] M. Isabel Collado,[‡] Alejandro Torrecillas,[§] J. C. Gómez-Fernández,[¶] Félix M. Goñi,[†] and Alicia Alonso[†]*

[†]Unidad de Biofísica (CSIC, UPV/EHU) and Departamento de Bioquímica and [‡]Servicio General de Resonancia Magnética Nuclear, Universidad del País Vasco, Bilbao, Spain; [§]Sección de Biología Molecular, Servicio de Apoyo a la Investigación, Universidad de Murcia; and [¶]Departamento de Bioquímica y Biología Molecular-A, Facultad de Veterinaria, Universidad de Murcia, Regional Campus of International Excellence "Campus Mare Nostrum", Murcia, Spain

ABSTRACT Sphingosine [(2S, 3R, 4E)-2-amino-4-octadecen-1, 3-diol] is the most common sphingoid long chain base in sphingolipids. It is the precursor of important cell signaling molecules, such as ceramides. In the last decade it has been shown to act itself as a potent metabolic signaling molecule, by activating a number of protein kinases. Moreover, sphingosine has been found to permeabilize phospholipid bilayers, giving rise to vesicle leakage. The present contribution intends to analyze the mechanism by which this bioactive lipid induces vesicle contents release, and the effect of negatively charged bilayers in the release process. Fluorescence lifetime measurements and confocal fluorescence microscopy have been applied to observe the mechanism of sphingosine efflux from large and giant unilamellar vesicles; a graded-release efflux has been detected. Additionally, stopped-flow measurements have shown that the rate of vesicle permeabilization increases with sphingosine concentration. Because at the physiological pH sphingosine has a net positive charge, its interaction with negatively charged phospholipids (e.g., bilayers containing phosphatidic acid together with sphingomyelins, phosphatidylethanolamine, and cholesterol) gives rise to a release of vesicular contents, faster than with electrically neutral bilayers. Furthermore, phosphorous 31-NMR and x-ray data show the capacity of sphingosine to facilitate the formation of nonbilayer (cubic phase) intermediates in negatively charged membranes. The data might explain the pathogenesis of Niemann-Pick type C1 disease.

INTRODUCTION

Sphingosine [(2S, 3R, 4E)-2-amino-4-octadecen-1, 3-diol], is the basic building block of sphingolipids and as a bioactive lipid it can exert its effects either through direct binding to enzymes (1) or indirectly through changes in membrane properties (2). This molecule behaves as a surface-active amphiphile with a critical micellar concentration of ~20 μM. The reported pK_a of sphingosine covers a range from 8.9 to 9.1 (3), to 6.6 (4), perhaps depending on the buffer or lipid environment. In addition, Sasaki et al. (4) indicate a pH-dependent structural transition in the sphingosine hydrogen bonding network from intra- to intermolecular as pH varies from 6.7 to 9.9. Assuming a partly cationic nature at neutral pH, sphingosine has been used in the preparation of positively charged liposomes for the study of membrane binding to a variety of macromolecules, including DNA and several enzymes (5). The unusual (in a lipid) net positive charge could also be biologically relevant when interacting with negatively charged phospholipids in membranes, because processes like pH-sensitive fusion (6) and the consequences of the formation of ion pairs by cationic and anionic lipids appear to be important in several cellular events (7). Also relevant in this context is the possible interest of electrostatic interaction between sphingosine and negatively charged lipids that can be particularly abundant in certain membranes, e.g., phosphatidylserine (PS) in the inner monolayer.

To our knowledge, a novel interesting property of sphingosine is its ability to permeabilize membranes to small solutes. This was shown using electrophysiological methods (8) and studying sphingosine-induced efflux of aqueous solutes from liposomes and ghost membranes (2). In the latter case the authors interpreted this effect as a result of the bilayer-rigidifying properties of sphingosine described previously (3). Rigidification would stabilize gel domains in membranes, raising their melting temperatures and increasing the transition cooperativity. Thus, the presence of coexisting gel and fluid domains in the plasma membrane would result in permeabilization.

More recent studies using giant unilamellar vesicles (GUVs) have revealed that sphingosine gives rise to different domain patterns depending on the surrounding lipid matrix. In a glycerophospholipid matrix sphingosine segregates in gel-like domains, in agreement with Contreras et al. (2), whereas cholesterol increases miscibility by melting the gel domains in a concentration-dependent manner (9). In this work, we pursue our studies on the mechanism of vesicle permeabilization by sphingosine and the differences between its interaction with neutral and negatively charged bilayers, which may be important for the explanation of some of its normal and pathological functions in the cell.

Submitted January 28, 2014, and accepted for publication April 23, 2014.

*Correspondence: alicia.alonso@ehu.es

Editor: Heiko Heerklotz.

0006-3495/14/06/2577/8 $2.00

http://dx.doi.org/10.1016/j.bpj.2014.04.038

MATERIALS AND METHODS

Materials

Sphingosine, sphingomyelin (SM), egg phosphatidic acid (PA), cholesterol, and the lipophilic fluorescent probe lissamine rhodamine-phosphatidylethanolamine (Rho-PE) were supplied by Avanti Polar Lipids (Alabaster, AL). Egg PE and PS were purchased from Lipid Products (South Nutfied, UK). Calcein (C0875) was from Sigma. The water-soluble dye 4,4-difluoro-1,3,5,7,8-pentamethyl-4-bora-3a,4a-diaza- *s*-indacene-2,6-disulfonic acid, disodium salt (BODIPY 492/515 disulfonate, D3238), 8-aminonaphtalene-1,3,6-trisulfonic acid (ANTS), and p-xylene-bis-pyridinium bromide (DPX) were supplied by Molecular Probes (Eugene, OR).

Methods

Vesicle preparation

Large unilamellar vesicles (LUVs) of diameters 100–150 nm were prepared by the extrusion method (10) using Nuclepore filters of 0.1 or 0.2 μm pore diameter, at a temperature above the transition temperature of the mixtures (40°C), in 10 mM HEPES, 150 mM NaCl, pH 7.4. For multilamellar (MLV) liposome preparation the lipids were dissolved in chloroform: methanol (2:1) and mixed in the required proportions, and the solvent was evaporated to dryness under a stream of nitrogen. Traces of solvent were removed by leaving the samples under high vacuum for at least 2 h. The samples were hydrated in 10 mM HEPES, 150 mM NaCl, pH 7.4 helping dispersion by stirring with a glass rod. The final phospholipid concentration of both LUV and MLV was measured in terms of lipid phosphorous (11).

Permeabilization assay in LUVs

Vesicle efflux was measured with the ANTS/DPX system (12). Calibration of these procedures has been described in detail previously (13,14). LUVs containing 12.5 mM ANTS, 45 mM DPX, 20 mM NaCl, and 10 mM HEPES were obtained by separating the unencapsulated material by gel filtration in a PD-10 desalting column that was eluted with 5 mM HEPES and 100 mM NaCl (pH 7.4). Fluorescence measurements were performed by setting the ANTS emission at 520 nm and the excitation at 355 nm. A cutoff filter (470 nm) was placed between the sample and the emission monochromator. The measurements were carried out in a FluoroMax-3 (Jobin Ybon, Horiba) spectrofluorometer.

Leakage mechanism

To find out whether partial leakage occurs as a result of an all-or-none event (some of the vesicles release all of their contents) or as a graded event (all of the vesicles release part of their contents) a method based on fluorescence lifetime measurements was applied (15). LUVs containing 70 mM calcein, 10 mM HEPES, and 0.5 mM EDTA (pH 7.4) were obtained by separating the unencapsulated material by gel filtration in a Sephacryl HR-500 column that was eluted with 10 mM HEPES, 0.5 mM EDTA, and 100 mM NaCl (pH 7.4). Aliquots with different liposome/sphingosine ratios were incubated at 37°C for 2 h. Fluorescence decays were measured using a FluoroMax-3 spectrofluorometer equipped with a time-correlated single photon counting (TCSPC) system (Jobin Ybon, Horiba) (excitation 467 nm, and emission 515 nm). Data analysis was performed using DAS 6 software (Jobin Ybon, Horiba). The decay curves were fitted with a biexponential model.

Stopped-flow kinetics

Leakage rate constants for increasing sphingosine concentrations were determined using a stopped-flow spectrofluorometer SFM-3 (BioLogic, France) where LUV composed of SM/PE/Ch (2:1:1) + 5 mol % PA (0.6 mM total lipids) and loaded with ANTS/DPX as explained previously (Permeabilization assay in LUVs), were mixed with sphingosine solutions of different concentrations in 1:1 volume proportions to a 0.3 mM final lipid concentration. Bio-Kine 32 v4.52 software was used for the measurements as well as for curve fitting and calculation of rate constants.

Permeabilization assay in GUVs

Giant vesicles were prepared using the electroformation method developed by Angelova and Dimitrov (1986). Vesicle observation was carried out at room temperature (22 ± 1°C) using a PRET-GUV 4 Chamber supplied by Industrias Técnicas ITC (Bilbao, Spain). Stock lipid solutions (0.2 mg/ml total lipid containing 0.4 mol % $DiIC_{18}$) were prepared in a chloroform/methanol (2:1, v/v) solution. 3 μL of the appropriate lipid stocks were added onto the surface of two platinum (Pt) electrodes and solvent traces removed by placing the chamber under high vacuum for 45 min. The chamber was then equilibrated at 50°C for 15 min and the Pt electrodes covered with 500 μl of a 200 mosm sucrose solution containing 10 mM HEPES (pH 7.4) in Milli Q water, previously equilibrated at 50°C. The Pt electrodes were connected to a generator (TG330 function generator, Thurlby Thandar Instruments, Huntingdon, UK) under AC field conditions 870 mV, 10 Hz at 50°C. The generator and water bath were then switched off and vesicles left to equilibrate for 30 min. Vesicles were then collected and 50 μl added to 250 μl of an equiosmolar glucose solution containing different concentrations of sphingosine and the water-soluble dye BODIPY 492/515 disulfonate, and then placed into a Micro-Incubator Platform DH-40i supplied by Warner Instruments (Hamden, CT). Sucrose-containing vesicles sedimented at the bottom of the chamber due to their higher density, which facilitated observation under the microscope. The chamber was placed in an inverted confocal fluorescence microscope (Nikon D-ECLIPSE C1, Nikon, Melville, NY). The excitation wavelength was 488 nm for the BODIPY and 561 nm for $DiIC_{18}$ and the images were collected using a bandpass filter of 515 ± 30 nm for BODIPY and 593 ± 40 nm for $DiIC_{18}$. Vesicles were left to equilibrate for 2 h at the desired temperature before image acquisition. Image treatment and quantitation was performed using the software EZ-C1 3.20 (Nikon).

Phosphorous 31-NMR (^{31}P-NMR)

60 mM lipid in the form of MLV was transferred to 5 mm NMR tubes. Data acquisition was performed in a Bruker AV500 spectrometer (Rheinstetten, Germany) operating at 202.45 MHz for ^{31}P with a 5 mm wideband probe and a gradient in the Z axis, at increasing temperatures. The data were recorded and processed with software TOPSPIN 1.3 (Bruker).

X-ray measurements

Simultaneous small and wide angle x-ray diffraction measurements were carried out using a modified Kratky compact camera (Hecus MBraum–Graz–Optical Systems, Graz, Austria), which uses two coupled linear position sensitive detectors (PSD, MBraun, Garching, Germany) to monitor the s-ranges ($s = 2\ \sin\theta/\lambda$, 2θ = scattering angle, $\lambda = 1.54$ Å) between 0.0075–0.07 and 0.20–0.29 $Å^{-1}$, respectively. Nickel-filtered Cu Kα x-rays were generated by a Philips PW3830 X-ray generator operating at 50 kV and 30 mA. The position calibration of the detectors was performed using Ag-stearate (small-angle region, d-spacing at 48.8 Å) and lupolen (wide-angle region, d-spacing at 4.12 Å) as reference materials. Samples for x-ray diffraction were prepared as multilamellar vesicles as described previously. The pellets were measured in a thin-walled high quality quartz capillary (1 mm diameter) held in a steel cuvette, which provides good thermal contact to the Peltier heating unit. X-ray diffraction profiles were obtained for 10 min exposure times after 10 min temperature equilibration. Data analysis and d-spacing calculations were performed with 3D-VIEW v4.1 software (Hecus MBraum, Graz, Austria).

RESULTS

Effect of PA on the rate of vesicle efflux induced by sphingosine

When LUV containing entrapped water-soluble fluorescent probes become permeable, the probes diffuse to the outer aqueous medium and this often leads to fluorescence changes that can be easily detected. To study the putative effect of the sphingosine positive charge on vesicle permeabilization either neutral or negatively charged LUVs were loaded with the fluorescence emitter/quencher couple ANTS/DPX. When permeabilization occurs, the complex is dissociated, ANTS fluorescence increases, and percent of leakage is calculated taking as 100% the fluorescence measured after addition of 15 μL 10% (w/v) Triton X-100. LUV composed of SM/PE/Ch (2:1:1 mol ratio) $\pm$ 5 mol % PA were treated with sphingosine (15 mol %) and the system allowed to reach an apparent equilibrium for 2 h.

Fig. 1 *A* shows an example of time courses of vesicle contents efflux after addition of sphingosine. The dose-response plots of sphingosine-induced vesicle efflux in electrically neutral vesicles composed of SM/PE/Ch (2:1:1), and in negatively charged vesicles composed of SM/PE/Ch (2:1:1) + 5 mol % PA can be seen in Fig. 1 *B*. The results under apparent equilibrium conditions (2 h treatment) show no significant differences for the extent of efflux between these two populations of vesicles. The results in the absence of PA are identical to those found by Contreras et al. (2).

Although no differences were detected in the extent of leakage, the results in Fig. 1, *C* and *D*, show that when the liposomes contain PA, the initial rate of release of vesicular contents is much faster than in the absence of PA. Furthermore, the apparent rate constant of the efflux increases with the sphingosine proportion, particularly in the case of the negatively charged bilayers.

Mechanism of vesicle contents release

Two different mechanisms of vesicle leakage have been described to explain the partial release of liposomal contents, namely the all-or-none mechanism in which some vesicles release all of their contents, or the graded mechanism in which all of the vesicles release part of their contents (16,17). Patel et al. (15) have described a membrane leakage assay based on time-resolved fluorescence decay curves, using calcein-loaded vesicles. Free calcein in a diluted solution has a fluorescence lifetime of $\tau = 4$ ns, whereas totally entrapped 70 mM calcein has a lifetime $\tau = 0.4$ ns. Theoretically, for an all-or-none leakage, calcein in the nonleaky vesicles retains a $\tau = 0.4$ ns and the empty vesicles do not contribute to the lifetime of entrapped calcein. Thus, the lifetime of entrapped dye should be constant at 0.4 ns irrespective of the global extent of release. In the graded mechanism, the more dye that has leaked out, the lower the concentration inside the vesicles, so the lifetimes of the entrapped dye should increase as the extent of leakage is increased. As seen in Fig. 2, the lifetime of the entrapped dye increases with sphingosine concentration, which reflects a graded mechanism. This is particularly clear for vesicles in the absence of PA. Patel et al. (15) suggest that a 20% efflux due to homogenous graded leakage should increase τ from 0.4 to 0.5 ns (see Fig. 3 and Eq. 2 in their work). This is in very good agreement with our observations.

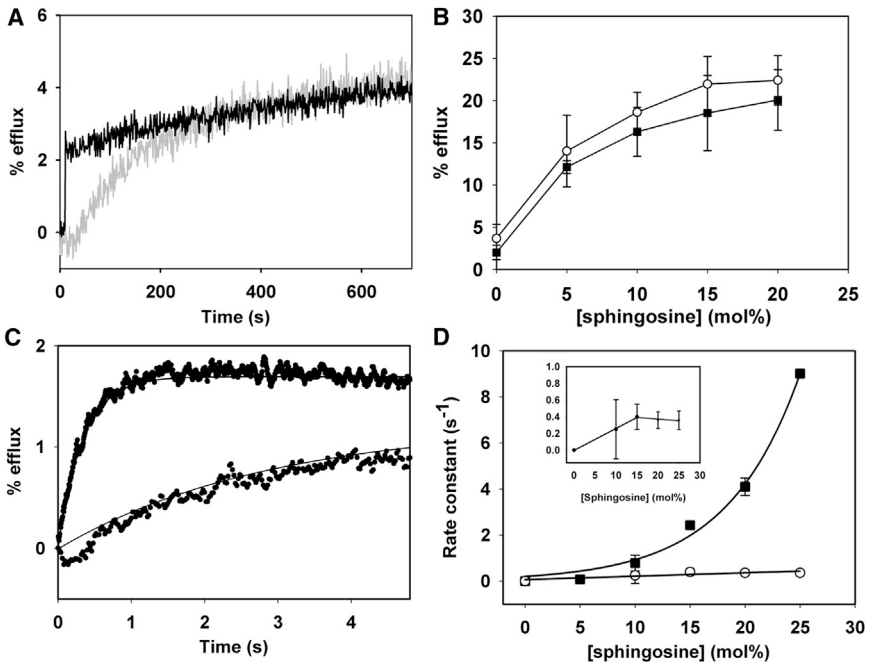

FIGURE 1 Effect of vesicle aqueous contents efflux induced by sphingosine on electrically neutral and negatively charged LUV. (*A*) Time course of 15 mol % sphingosine-induced vesicle leakage. Vesicle composition was SM/PE/Ch (2:1:1) with (*black trace*) or without (*gray trace*) 5 mol % PA. (*B*) Extent of leakage under steady-state conditions. (○) SM/PE/Ch (2:1:1) (■) SM/PE/Ch (2:1:1) + 5 mol % PA. (*C*) Time course of leakage. Early stages of sphingosine-induced efflux of vesicular contents. Vesicle efflux induced by 15 mol % sphingosine. (*D*) Rate constants of vesicle efflux kinetics induced by increasing sphingosine concentrations. The PA line was fitted to a monoexponential curve ($r^2 = 0.984$). Inset: rates in the absence of PA, *Y*-axis expanded.

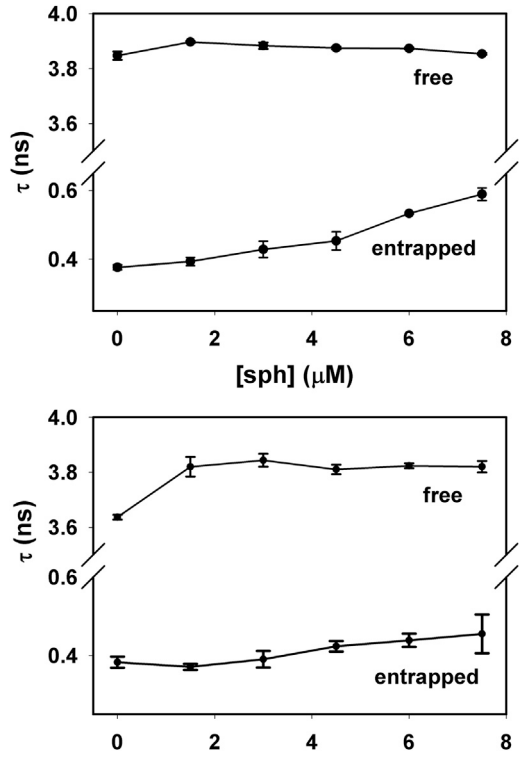

FIGURE 2 Fluorescence lifetime data of sphingosine-induced membrane leakage. 30 μM LUV, 2 h incubation. The data correspond to the lifetime of free calcein ($\approx$4 ns) and entrapped calcein ($\approx$0.4 ns) (*A*) LUVs composed of SM/PE/Ch (2:1:1). (*B*) LUVs composed of SM/PE/Ch (2:1:1) + 5 mol % PA.

To ensure that in both cases sphingosine promotes vesicle permeabilization by a graded mechanism, single vesicle analysis was carried out using confocal microscopy of GUV (18). Fig. 3 is a representative example of the observed graded mechanism in which GUVs composed of SM/PE/Ch (2:1:1) are incubated for 2 h without and with 1.4 μM sphingosine. For the experiments in Fig. 3, entrance of the soluble probe BODIPY 492/515 disulfonate to the GUVs was measured by confocal microscopy, and the extent of permeabilization was normalized with respect to the external fluorescence. Fig. 3 *C* shows the dose-dependent vesicle permeabilization induced by sphingosine, as observed using the GUV/confocal microscopy method. Fig. 4 shows the distribution of filling degrees for the individual vesicles in the ensemble of GUVs composed of SM/PE/Ch (2:1:1) without (Fig. 4 *A*) or with 5 mol % PA (Fig. 4 *B*). Again, both graphs show a graded mechanism with vesicles that exhibit a partial permeabilization in which the percent dye inside increases in parallel with the concentration of sphingosine. For comparison see Apellániz et al. (18), where the same plot is used to show both mechanisms, graded and all-or-none. In the all-or-none case, two main peaks are found at 0% and 100% filling.

The graded mechanism is related to the effect of membrane destabilization induced by sphingosine in contrast to the all-or-none mechanism, the latter more likely related to pores characterized by a sufficiently long lifetime to allow equilibration of the probe with the external medium. No differences in mechanism are found between neutral and negatively charged vesicles showing that the differences in the rate of permeabilization are not due to a different permeabilization mechanism.

Effect of sphingosine on the phase behavior of negatively charged vesicles

To obtain a further insight into the mechanism of sphingosine-induced membrane permeabilization, ^{31}P-NMR spectroscopy was applied to samples (MLV) composed of SM/PE/Ch (2:1:1) with or without 20 mol % PA, to which 20 mol % sphingosine had been added. ^{31}P-NMR can provide information on the phase structure of lipids in aqueous dispersions (19). 20 mol % PA was used in our structural studies to facilitate observation of changes in lipid architecture.

At 25°C, both in the absence and presence of PA (Fig. 5) the spectral line shape is asymmetric, with a shoulder at the low-frequency side, typical of the lamellar phase (19). In the absence of PA (Fig. 5 *A*) the structure remains lamellar in a wide range of temperatures (25–85°C). The two P nuclei, from SM and PE, are only partially resolved under these conditions. However, when 20 mol % PA is included in vesicles composed of SM/PE/Ch (2:1:1, mol ratio) an isotropic signal appears at and above 65°C (Fig. 5 *B*). Lipid samples are often heated up in ^{31}P-NMR experiments to facilitate any spontaneous, though slow, tendency of the lipids to adopt a nonlamellar phase (20). ^{31}P-NMR spectra such as shown in Fig. 5 *B* were performed in the absence of sphingosine. Under those conditions the sample remained lamellar in the 25–85°C range (data not shown). We conclude that both sphingosine and PA are required for the formation of nonlamellar phases.

Thus, it appears as if the sphingosine-PA (presumably electrostatic) interaction tends to destabilize the bilayer. To see if this effect was not only seen in the presence of PA but also with other negatively charged phospholipids, similar experiments were carried out including PS in the mixture instead of PA (Fig. 6). An isotropic signal is also detected meaning that the formation of this nonlamellar structure is not only due to the specific structure of PA but to its net negative charge. An isotropic ^{31}P-NMR signal can be originated by a variety of structures, namely very small vesicles, micelles, or cubic phases. Distinguishing between the various possibilities requires the use of different techniques.

Sphingosine induces formation of an inverted cubic phase upon interaction with negatively charged bilayers

The ability of lipids to form cubic phases in aqueous dispersions has been known for a long time (21). Furthermore,

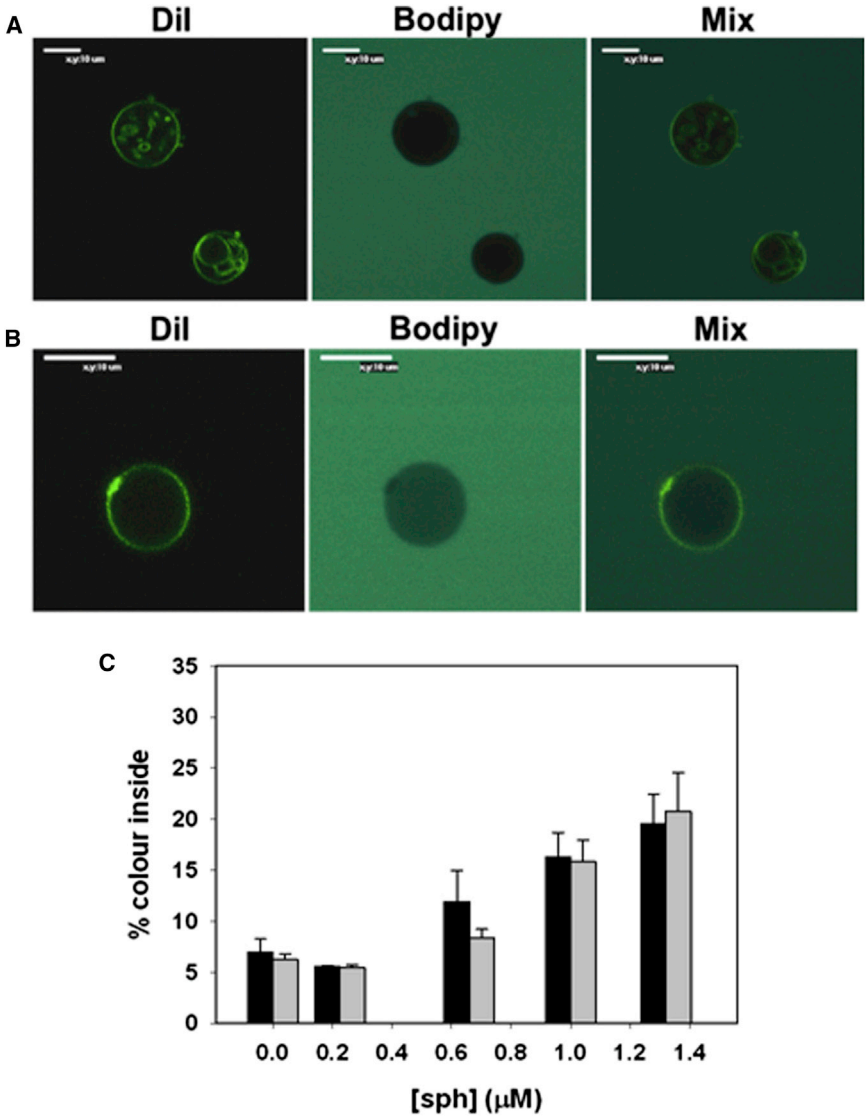

FIGURE 3 Confocal fluorescence microscopy images of GUVs after 2 h incubation in buffer containing BODIPY 492/515. (*A*) SM/PE/Ch (2:1:1) + buffer. (*B*) SM/PE/Ch (2:1:1) + 1.4 μM sphingosine. (*C*) Assay of sphingosine-induced influx of BODIPY into GUV ($t = 2$ h). Black bars: SM/PE/Ch (2:1:1), gray bars: SM/PE/Ch (2:1:1) + 5 mol % PA. Average values $\pm$ S.D. of 90 vesicles. To see this figure in color, go online.

these nonlamellar structures are believed to be involved in various cellular processes such as fusion or fission events (22–27). Thus, characterizing the ability of membrane lipids to form these structures has been a topic of long-standing interest (28). X-ray diffraction is the most important and least ambiguous method of structural determination of lipid phases, and it can be used to distinguish if an isotropic signal found by NMR is due to the formation of a micellar or a cubic phase. For this reason, in this study MLV samples with the same composition as the ones in NMR experiments (Fig. 5, *A* and *B*), were examined in x-ray capillaries as detailed in the Methods section.

Temperature among others is an important variable for the polymorphism of lipid-water systems, therefore to facilitate observation of cubic phases the samples were subjected to thermal cycles 20-95-20°C (28,20), and as in NMR experiments, measurements were taken at increasing temperatures. As seen in Fig. 7, a cubic phase was induced in the presence of PA (Fig. 7 *B*) but not in its absence (Fig. 7 *A*). In the absence of PA (Fig. 7 *A*) only in the sample at 20°C are there enough reflections to diagnose the phase. The three reflections appear approximately at distances 1, 1/2, 1/4, characteristic of a lamellar phase, in agreement with ^{31}P-NMR data. In Fig. 7 *B* the main scattering maximum is around 70 Å, and the subsequent reflections occur at 1, $1/\sqrt{2}$, $1/\sqrt{4}$. This sequence is characteristic of a cubic phase, and could be correlated to either Q^{223} (Pm3n) or Q^{229} (Im3m) cubic phase. However, it has been impossible in this study to distinguish between these two inverted cubic phases due to instrumental limitations.

DISCUSSION

Sphingosine is known to have apoptotic and antiproliferative effects in cells and these effects are the overall result of a large number of direct and indirect inhibitory and

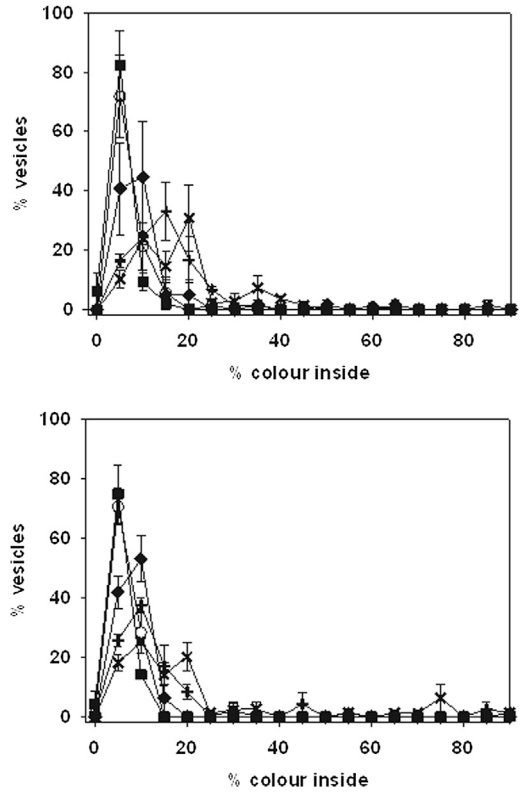

FIGURE 4 The distribution of GUVs as a function of the degree of filling after 2 h incubation with sphingosine is shown in GUVs made of (*A*) SM/PE/Ch (2:1:1) and (*B*) SM/PE/Ch (2:1:1) + 5% PA. Sphingosine concentration: (○) 0 μM, (X) 0.2 μM, (◆) 0.6 μM, (✚) 1 μM, (×) 1.3 μM. Average values ± SD of 90 vesicles.

stimulatory interactions with enzymes (30). Sphingosine-dependent modulation of enzyme activity can be the result of direct lipid-protein interactions, but also occur secondarily to membrane effects of sphingosine. This simple sphingolipid has been shown to increase membrane permeability to solutes (2,8). Siskind et al. (8) proposed that sphingosine acted through formation of channels in the membrane, whereas Contreras et al. (2) suggested that the sphingolipid would rigidify membrane domains so that solutes would diffuse through the interdomain structural defects. The results in this work help in the interpretation of these and other results.

A net positive charge of sphingosine has commonly been assumed because of the amino group in C2 (5), however this view has been challenged by Sasaki et al. (4) who, on the basis of NMR studies, suggested that the pK of the sphingosine amino group in bilayers could be as low as 6.6, depending on lipid composition. Acid-base properties of sphingolipids are known to be dependent on the phospholipid environment (31). Although we have not addressed specifically this point, the results in this work (Figs. 1, *C* and *D*, 5, 6, 7), clearly indicate that sphingosine under our conditions is at least partly protonated, because of its different effects on neutral and negatively charged bilayers.

Two kinds of results in this work help in clarifying the mechanism of sphingosine-dependent vesicle efflux of aqueous contents. First, the data in Figs. 2 and 4 provide two independent proofs that contents are released in a graded way, as opposed to an all-or-none mechanism (14–17). A graded mechanism does not agree well with the channel hypothesis of vesicle leakage proposed by Siskind et al. (8). A channel would give rise to a rapid and complete release of contents, i.e., an all-or-none event.

Second, the structural studies shown in Figs. 5–7 support the possibility that, at least when interacting with negatively charged bilayers, sphingosine is inducing formation of nonlamellar structures in the vesicles. The ^{31}P-NMR and x-ray data describe extensive and long-lived events in which virtually all of the lamellar phase is transformed into an isotropic, apparently cubic phase. This should probably be interpreted at the physiological temperature as a tendency to form localized and transient disruptions of the bilayer. Formation of nonbilayer structures would lead in turn to a

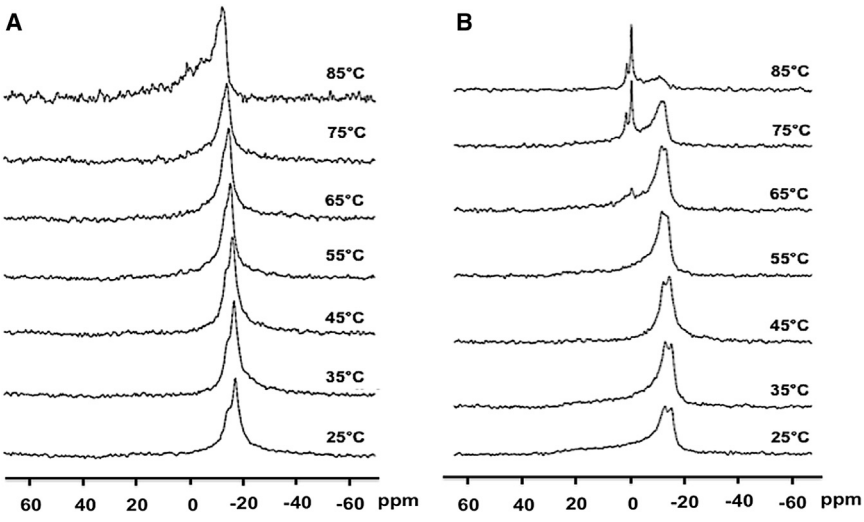

FIGURE 5 ^{31}P-NMR spectra as a function of temperature of the mixture SM/PE/Ch (2:1:1) + 20 mol % sphingosine. (*A*) Without PA and (*B*) with 20 mol % PA.

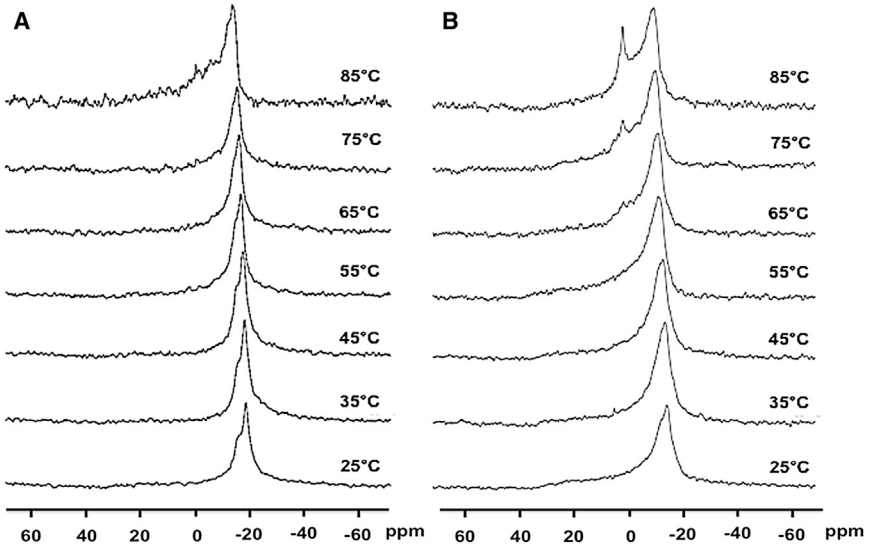

FIGURE 6 ^{31}P-RMN spectra as a function of temperature of the mixture SM/PE/Ch (2:1:1) + 20 mol % sphingosine. (*A*) Without PS and (*B*) with 20 mol % PS.

faster transfer of solutes in the presence of negatively charged phospholipids as the leakage rate constants show. Furthermore, this sort of transient effects would be in agreement with the observed graded release. The proposed mechanism of gel domain rigidification to explain sphingosine-induced permeability (2,9) remains probably valid for the case of electrically neutral bilayers. Recently published data appear to confirm this hypothesis (32). However, in the presence of negatively charged membrane surfaces, as commonly found inside the cell, nonlamellar phase formation should also be considered as an additional or alternative mechanism. It has been reported (7) that upon interaction between a cationic and an anionic lipid in the endosomal membrane, non-lamellar structures can be formed, which could in turn disrupt the membrane. A similar mechanism might be operating in our system. Note that the inner leaflet of the plasma membrane is highly enriched in negatively charged lipids, thus could be a target for the permeability effect of sphingosine. Formation of nonlamellar structures, particularly of an inverted cubic phase, can only happen starting with several adjacent layers, and not from a single bilayer. In our leakage assay vesicles are unilamellar, but vesicle aggregation phenomena cannot be excluded, neither here nor in the cell environment, that can operate as the seeds for nonlamellar phase formation. Ghosh et al. (33) indicated that sphingosine derivatives, e.g., sphingosine-1-phosphate, would mediate calcium release from intracellular stores into the cytosol. Our data suggest that sphingosine itself may be responsible for the calcium efflux. Under healthy conditions the steady-state concentration of free sphingosine in cell membranes is negligible, however either by de novo synthesis or through the action of ceramidase, sphingosine concentrations may increase significantly for a short time in a given region of the membrane. It is under those transient conditions when sphingosine could modify membrane permeability

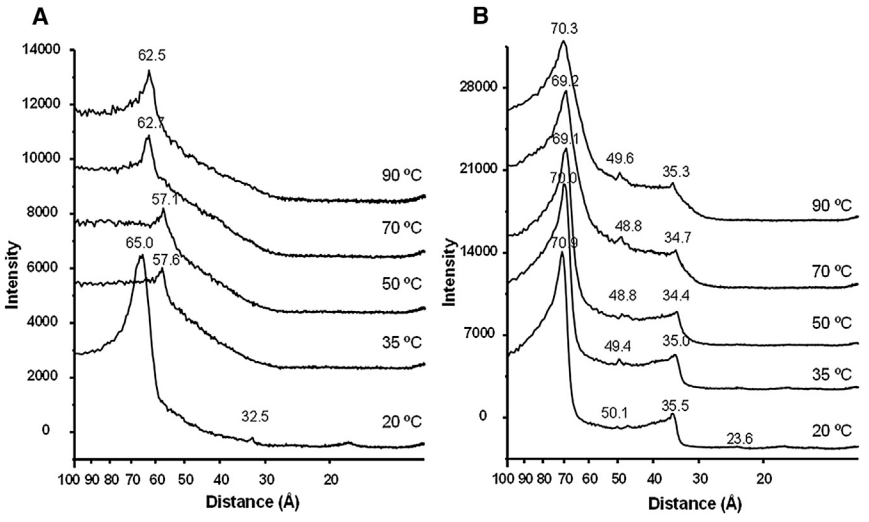

FIGURE 7 Small angle x-ray scattering of aqueous dispersions of SM/PE/Ch (2:1:1) + 20 mol % sphingosine, (*A*) without PA and (*B*) with 20 mol % PA.

as described in this work, before being reincorporated into more complex sphingolipids, or degraded.

Niemann-Pick disease type C1 is a sphingosine storage disease that causes calcium depletion in lysosomes and late endosomes (34). These membranes are rich in negatively charged lipids, particularly PI (3,5) P2, and lysobisphosphatidic acid (35). Our data provide a possible pathogenic mechanism for the sphingosine-induced calcium deregulation in this disease.

In summary, the previous data support the idea that sphingosine impairs the membrane permeability barrier through the generation of structural defects, either by rigidifying certain domains or, in the case of negatively charged bilayers, by inducing transient nonlamellar structures. This should give rise to a graded, rather than an all-or-none, efflux of vesicle aqueous contents. Under the conditions of the Niemann-Pick disease type C1 sphingosine would cause the observed calcium release from lysosomes and late endosomes via the mechanisms described in this work.

The authors thank E. E. Kooijman and D.M. Agra-Kooijman for their help with preliminary X-ray measurements.

This work was supported in part by grants from the Spanish Ministry of Economy (BFU 2012-34885; BFU 2011-28566) and the Basque Government (IT838-13; IT849-13). N.J.R. was a predoctoral student supported by the Basque Government.

REFERENCES

1. Hannun, Y. A., C. R. Loomis, …, R. M. Bell. 1986. Sphingosine inhibition of protein kinase C activity and of phorbol dibutyrate binding in vitro and in human platelets. *J. Biol. Chem.* 261:12604–12609.
2. Contreras, F. X., J. Sot, …, F. M. Goñi. 2006. Sphingosine increases the permeability of model and cell membranes. *Biophys. J.* 90:4085–4092.
3. López-García, F., V. Micol, …, J. C. Gómez-Fernández. 1993. Interaction of sphingosine and stearylamine with phosphatidylserine as studied by DSC and NMR. *Biochim. Biophys. Acta.* 1153:1–8.
4. Sasaki, H., H. Arai, …, S. H. White. 2009. pH dependence of sphingosine aggregation. *Biophys. J.* 96:2727–2733.
5. Mustonen, P., J. Lehtonen, …, P. K. J. Kinnunen. 1993. Effects of sphingosine on peripheral membrane interactions: comparison of adriamycin, cytochrome *c*, and phospholipase A2. *Biochemistry.* 32:5373–5380.
6. Hafez, I. M., S. Ansell, and P. R. Cullis. 2000. Tunable pH-sensitive liposomes composed of mixtures of cationic and anionic lipids. *Biophys. J.* 79:1438–1446.
7. Semple, S. C., A. Akinc, …, M. J. Hope. 2010. Rational design of cationic lipids for siRNA delivery. *Nat. Biotechnol.* 28:172–176.
8. Siskind, L. J., S. Fluss, …, M. Colombini. 2005. Sphingosine forms channels in membranes that differ greatly from those formed by ceramide. *J. Bioenerg. Biomembr.* 37:227–236.
9. Georgieva, R., K. Koumanov, …, G. Staneva. 2010. Effect of sphingosine on domain morphology in giant vesicles. *J. Colloid Interface Sci.* 350:502–510.
10. Mayer, L. D., M. J. Hope, and P. R. Cullis. 1986. Vesicles of variable sizes produced by a rapid extrusion procedure. *Biochim. Biophys. Acta.* 858:161–168.
11. Bartlett, G. R. 1959. Phosphorus assay in column chromatography. *J. Biol. Chem.* 234:466–468.
12. Ellens, H., J. Bentz, and F. C. Szoka. 1985. H+- and Ca2+-induced fusion and destabilization of liposomes. *Biochemistry.* 24:3099–3106.
13. Goñi, F. M., J. L. Nieva, …, A. Alonso. 1994. Phospholipase-C-promoted liposome fusion. *Biochem. Soc. Trans.* 22:839–844.
14. Nieva, J. L., F. M. Goñi, and A. Alonso. 1989. Liposome fusion catalytically induced by phospholipase C. *Biochemistry.* 28:7364–7367.
15. Patel, H., C. Tscheka, and H. Heerklotz. 2009. Characterizing vesicle leakage by fluorescence lifetime measurements. *Soft Matter.* 5:2849–2851.
16. Ostolaza, H., B. Bartolomé, …, F. M. Goñi. 1993. Release of lipid vesicle contents by the bacterial protein toxin alpha-haemolysin. *Biochim. Biophys. Acta.* 1147:81–88.
17. Parente, R. A., S. Nir, and F. C. Szoka, Jr. 1990. Mechanism of leakage of phospholipid vesicle contents induced by the peptide GALA. *Biochemistry.* 29:8720–8728.
18. Apellániz, B., J. L. Nieva, …, A. J. García-Sáez. 2010. All-or-none versus graded: single-vesicle analysis reveals lipid composition effects on membrane permeabilization. *Biophys. J.* 99:3619–3628.
19. Cullis, P. R., and B. De Kruijff. 1978. Polymorphic phase behaviour of lipid mixtures as detected by 31P NMR. Evidence that cholesterol may destabilize bilayer structure in membrane systems containing phosphatidylethanolamine. *Biochim. Biophys. Acta.* 507:207–218.
20. Shyamsunder, E., S. M. Gruner, …, C. P. Tilcock. 1988. Observation of inverted cubic phase in hydrated dioleoylphosphatidylethanolamine membranes. *Biochemistry.* 27:2332–2336.
21. Luzzati, V., A. Tardieu, and T. Gulik-Krzywicki. 1968. Polymorphism of lipids. *Nature.* 217:1028–1030.
22. Goñi, F. M., and A. Alonso. 1999. Structure and functional properties of diacylglycerols in membranes. *Prog. Lipid Res.* 38:1–48.
23. Nieva, J. L., A. Alonso, …, V. Luzzati. 1995. Topological properties of two cubic phases of a phospholipid:cholesterol:diacylglycerol aqueous system and their possible implications in the phospholipase C-induced liposome fusion. *FEBS Lett.* 368:143–147.
24. Nieva, J. L., F. M. Goñi, and A. Alonso. 1993. Phospholipase C-promoted membrane fusion. Retroinhibition by the end-product diacylglycerol. *Biochemistry.* 32:1054–1058.
25. Ruiz-Argüello, M. B., G. Basáñez, …, A. Alonso. 1996. Different effects of enzyme-generated ceramides and diacylglycerols in phospholipid membrane fusion and leakage. *J. Biol. Chem.* 271:26616–26621.
26. Siegel, D. P. 1984. Inverted micellar structures in bilayer membranes. Formation rates and half-lives. *Biophys. J.* 45:399–420.
27. Walter, A., P. L. Yeagle, and D. P. Siegel. 1994. Diacylglycerol and hexadecane increase divalent cation-induced lipid mixing rates between phosphatidylserine large unilamellar vesicles. *Biophys. J.* 66:366–376.
28. Tenchov, B., and R. Koynova. 2012. Cubic phases in membrane lipids. *Eur. Biophys. J.* 41:841–850.
29. Reference deleted in proof.
30. Birbes, H., S. El Bawab, …, Y. A. Hannun. 2002. Mitochondria and ceramide: intertwined roles in regulation of apoptosis. *Adv. Enzyme Regul.* 42:113–129.
31. Kooijman, E. E., J. Sot, …, F. M. Goñi. 2008. Membrane organization and ionization behavior of the minor but crucial lipid ceramide-1-phosphate. *Biophys. J.* 94:4320–4330.
32. Zupancic, E., A. C. Carreira, …, L. C. Silva. 2014. Biophysical implications of sphingosine accumulation in membrane properties at neutral and acidic pH. *J. Phys. Chem. B*. http://dx.doi.org/10.1021/jp501167f.
33. Ghosh, T. K., J. Bian, and D. L. Gill. 1990. Intracellular calcium release mediated by sphingosine derivatives generated in cells. *Science.* 248:1653–1656.
34. Lloyd-Evans, E., A. J. Morgan, …, F. M. Platt. 2008. Niemann-Pick disease type C1 is a sphingosine storage disease that causes deregulation of lysosomal calcium. *Nat. Med.* 14:1247–1255.
35. Gruenberg, J. 2003. Lipids in endocytic membrane transport and sorting. *Curr. Opin. Cell Biol.* 15:382–388.